Primary Populations of Metastable Antiprotonic ^{4}He and ^{3}He Atoms

M. Hori,[1] J. Eades,[1] R. S. Hayano,[2] T. Ishikawa,[2] J. Sakaguchi,[2] T. Tasaki,[2] E. Widmann,[2] H. Yamaguchi,[2] H. A. Torii,[3] B. Juhász,[4] D. Horváth,[5] and T. Yamazaki[6]

[1]*CERN, CH-1211 Geneva 23, Switzerland*
[2]*Department of Physics, University of Tokyo, 7-3-1 Hongo, Bunkyo-ku, Tokyo 113-0033, Japan*
[3]*Institute of Physics, University of Tokyo, Komaba, Meguro-ku, Tokyo 153-8902, Japan*
[4]*Institute of Nuclear Research of the Hungarian Academy of Sciences, H-4001 Debrecen, Hungary*
[5]*KFKI Research Institute for Particle and Nuclear Physics, H-1525 Budapest, Hungary*
[6]*RI Beam Science Laboratory, RIKEN, Wako, Saitama 351-0198, Japan*

(Received 8 December 2001; published 7 August 2002)

Initial distributions of metastable antiprotonic ^{4}He and ^{3}He atoms over principal (n) and angular momentum (ℓ) quantum numbers have been deduced using laser spectroscopy experiments. The regions $n = 37$–40 and $n = 35$–38 in the two atoms account for almost all of the observed fractions [$(3.0 \pm 0.1)\%$ and $(2.4 \pm 0.1)\%$] of antiprotons captured into metastable states.

DOI: 10.1103/PhysRevLett.89.093401 PACS numbers: 36.10.–k, 25.43.+t, 34.90.+q

A negatively charged particle X^- (such as μ^-, π^-, or $\overline{p}$) approaching an atom at electron-volt energies can displace one of its electrons, thereby forming an exotic atom [1]. Little is known about the principal (n) and angular momentum (ℓ) quantum numbers of the atom's primordial (i.e., initially occupied) states. It has been widely believed since the 1950s [2–4] that in exotic hydrogen and helium atoms, n will be distributed around the value

$$n \sim n_0 = \sqrt{M^*/m_e} \tag{1}$$

(M^* being the reduced mass of the X^--nucleus system, and m_e the electron mass), which corresponds to the X^- orbital with the same radius and binding energy as that of the displaced $1s$ electron. In this paper, we describe measurements of the (n, ℓ) distributions of antiprotons captured into atomic states in metastable antiprotonic helium [5–8], including the isotopes $\overline{p}\,^4\mathrm{He}^+$ for which $n_0 = 38.3$ and $\overline{p}\,^3\mathrm{He}^+$ for which $n_0 = 37.1$.

These $\overline{p}\mathrm{He}^+$ states (see Fig. 1) have microsecond-scale lifetimes against annihilation, because their large ℓ values ($\ell \sim n - 1$) do not permit them to deexcite by Auger emission of the electron. Instead, the atoms slowly undergo a series of constant $v = n - \ell - 1$ radiative transitions (i.e., $\Delta n = \Delta\ell = -1$). They finally reach states which proceed rapidly to $\overline{p}\mathrm{He}^{2+}$ ions, which are immediately destroyed by collisional Stark effects. So far, the numbers of antiprotons populating two metastable states in $\overline{p}\,^4\mathrm{He}^+$ [namely, $(n, \ell) = (39, 35)$ and $(37, 34)$] have been measured [9,10] using laser spectroscopic methods [11] at the former LEAR facility at CERN. The two states represent only a small fraction of the totality of metastable states shown in Fig. 1; moreover, since for technical reasons [9] the populations could be measured only after a minimum delay of $t = 1.8$ μs following atomic formation, the primary populations (those at $t = 0$) could not be reliably estimated. We study here a total of 20 transitions in $\overline{p}\,^4\mathrm{He}^+$ and $\overline{p}\,^3\mathrm{He}^+$ atoms starting at $t = 300$ ns, and estimate the primary populations in nearly all the metastable states.

These experiments were made at the Antiproton Decelerator at CERN, the setup [12] being an extension of our former one. Metastable $\overline{p}\mathrm{He}^+$ atoms were produced

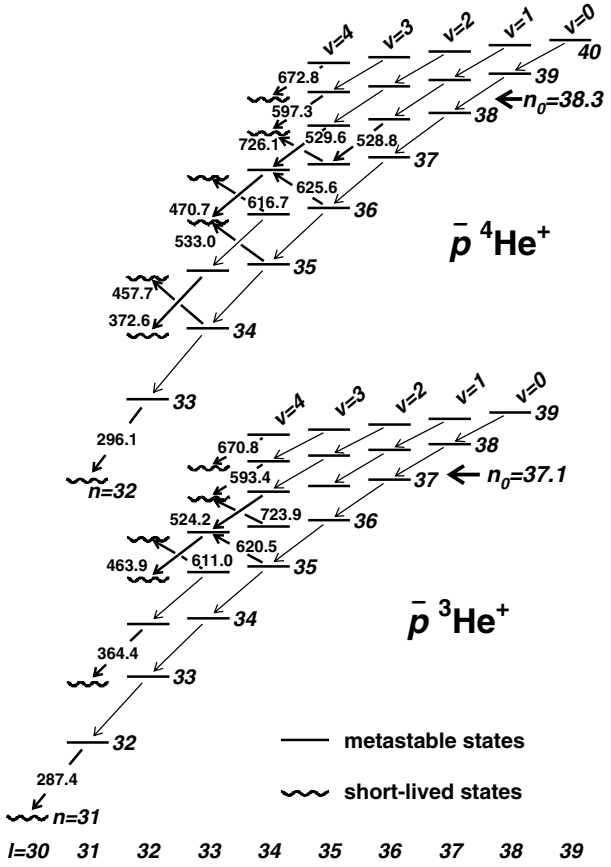

FIG. 1. Energy level diagrams of $\overline{p}\,^4\mathrm{He}^+$ and $\overline{p}\,^3\mathrm{He}^+$ atoms. Wavelengths of the studied transitions are indicated in nanometers. The one at $\lambda = 670.8$ nm was not observed.

 0031-9007/02/89(9)/093401(4)$20.00

by injecting a 200-ns-long pulse of 4×10^7 antiprotons into a cryogenic target, containing either ^{4}He (of purity 99.9999%) or ^{3}He (99.997%) gas, at temperatures $T = 5.5$–6.2 K and pressures $P = 0.2$–0.4 bar [corresponding to an atomic density $\rho = (2 - 5) \times 10^{20}$ cm^{-3}]. By detecting the charged pions produced in the annihilation with Cherenkov counters, a delayed annihilation time spectrum (the spectrum of intervals between an antiproton arrival in the target and its annihilation) could be obtained. The atoms were irradiated by a resonant laser pulse at time t_1, which induced transitions between adjacent pairs of metastable and short-lived states, thereby forcing the annihilations of the antiprotons populating the metastable member of the two [11]. This superimposed a sharp spike on the delayed annihilation time spectrum [see Figs. 2(a)–2(c)]. A dye laser pumped by a Nd:YAG laser was used to produce laser pulses with wavelengths of $\lambda = 287.4$–726.1 nm, bandwidths of 3 GHz, pulse lengths of 5 ns, and power densities of 4–40 mJ/cm^2. This was enough to saturate typical transitions with dipole moments of 0.03–0.3 D, and maximize the intensity in the annihilation spike at t_1. By varying the timing of the laser pulse between $t_1 = 0.3$ and 16 μs and measuring the spike intensity at each t_1, the population $P_{(n,\ell)}(t_1)$ (i.e., the number of antiprotons populating the parent state at t_1, normalized to the total number of antiprotons stopped in the target) could be obtained. The experimental background consisted mostly of pions stopping in the material around the target and undergoing $\pi \rightarrow \mu \rightarrow e$ decay [13], the contribution of which was estimated using Monte Carlo simulations.

Measurements were made for the 12 transitions in $\overline{p}\,^4$He$^+$ shown in Fig. 1, and eight transitions in $\overline{p}\,^3$He$^+$ (excluding the one at $\lambda = 670.8$ nm which could not be detected). The 529.6-nm and 625.6-nm transitions in $\overline{p}\,^4$He$^+$ are between metastable states and usually cannot be observed; here we resolved them at target densities $\rho = 2 \times 10^{21}$ cm^{-3}, where the resonance daughter state (37, 34) common to both transitions became short-lived due to collisional effects [14]. Similarly, the 524.2-nm and 620.5-nm transitions in $\overline{p}\,^3$He$^+$ were measured in ^{3}He targets at $\rho = 1 \times 10^{21}$ cm^{-3}, where the lifetime of the state (36, 33) was shortened to $\tau \sim 60$ ns [15]. The population in the state (38, 36) in $\overline{p}\,^4$He$^+$ was probed by irradiating the atoms with two successive laser pulses, the first inducing the transition $(38, 36) \rightarrow (37, 35)$ at $\lambda = 528.8$ nm and the second (10 ns later) the transition $(37, 35) \rightarrow (38, 34)$ at 726.1 nm. The resulting annihilation spike thus contained antiprotons which populated both the (38, 36) and the (37, 35) states. We derived the primary populations $P_{(n,\ell)}(t = 0)$ by extrapolating the measured population evolutions to $t = 0$. These were relatively insensitive to density between $\rho = 2 \times 10^{20}$ and 2×10^{21} cm^{-3}. The statistical and systematic experimental errors on $P_{(n,\ell)}(t = 0)$ varied between (5–20)% and (15–30)%, respectively, depending on the transition. The estimated primary populations differ from those of previous experiments [9,10] by a factor of 3–5, primarily due to the new information at early ($t < 1.8$ μs) times.

The state (40, 35) in $\overline{p}\,^4$He$^+$ [see Fig. 3(a)] was found to have a primary population of (0.10 ± 0.02)%. This population decreased with a 1-μs time constant, which indicates that very few metastable atoms occupy the region $n \geq 41$ in the $\upsilon = 4$ cascade. The population in (39, 35) decreased with a lifetime of 1.9 μs; this value (which is longer than the $\tau_{(39,35)} = 1.4$-μs lifetime of that state [14]) results when the antiprotons initially occupying (40, 36) deexcite into (39, 35), and thus increase the population in the latter state. The corresponding lifetimes of (38, 35) and (38, 36)

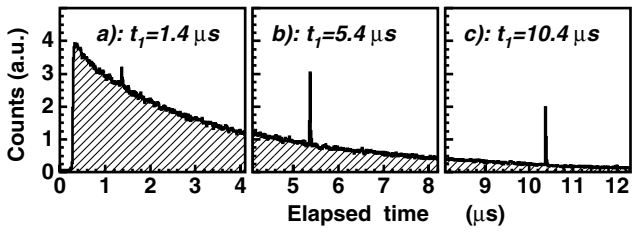

FIG. 2. Three delayed annihilation time spectra of $\overline{p}\,^4$He$^+$ with annihilation spikes of the transition $(n, \ell) = (33, 32) \rightarrow (32, 31)$ induced at $t_1 = 1.4$ μs (a), 5.4 μs (b), and 10.4 μs (c).

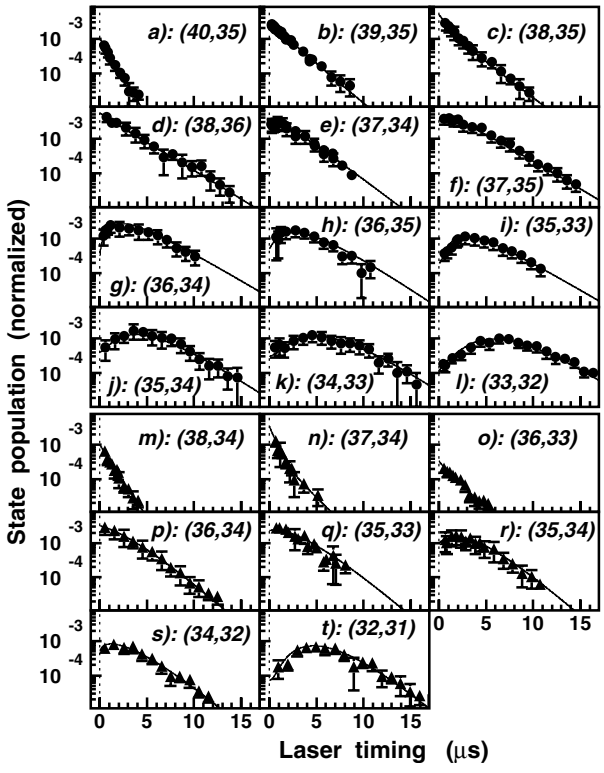

FIG. 3. Time evolutions of the populations in 12 $\overline{p}\,^4$He$^+$ [filled circles with error bars in (a)–(l)] and eight $\overline{p}\,^3$He$^+$ [filled triangles in (m)–(t)] states. The best fit of a cascade model is shown in solid lines.

were still longer (~ 2.2 μs), due to spontaneous deexcitation from (39, 36) and (39, 37). The populations in (37, 34) and (37, 35) decreased with 3-μs-lifetimes, and had downward-bending profiles at early times caused by the large feeding from (38, 35) and (38, 36).

In contrast, very small primary populations were found in $\overline{p}\,^4\mathrm{He}^+$ states with $n \leq 36$. These populations increased [see Figs. 3(g)–3(l)] as antiprotons deexcited from higher, initially populated states, reaching a maximum at progressively later times $t_{\max}$ with decreasing n. The longest-living antiprotons were found in the lowest metastable state (33,32) in the $\upsilon = 0$ cascade; since antiprotons captured in the $n \sim 38$ regions made 6–7 radiative transitions before reaching this state, a significant population ($\sim 0.01\%$) could be observed even at $t_1 = 16$ μs. The primary populations in the states (37, 36) and above in the $\upsilon = 0$ cascade were estimated by fitting cascade models on the population evolution of the state (36, 35).

In $\overline{p}\,^3\mathrm{He}^+$ atoms [see Figs. 3(m)–3(t)], the population in the state (38, 34) decreased with a 1.0-μs lifetime which (being similar to the theoretical state lifetime of $\tau_{(38,34)} =$ 1.0 μs [16,17]) indicates that the populations in the region $n \geq 39$ in the $\upsilon = 3$ cascade are very small. The last transition (39, 34) $\rightarrow$ (38, 33) in the $\upsilon = 4$ cascade at $\lambda =$ 670.8 nm was searched for, but could not be detected, which shows the populations in this cascade are also negligible. The largest populations [$P_{(n,\ell)}(t = 0) \sim 0.3\%$] were found in the states (36, 34), (36, 35), (37, 34), (37, 35), and (37, 36). In contrast to the $\overline{p}\,^4\mathrm{He}^+$ case, significant primary populations were detected even in low-n regions, with the lowest metastable state in the $\upsilon = 1$ cascade having a value of $P_{(34,32)}(t = 0) = (0.06 \pm 0.02)\%$. The lowest state (32, 31) in the $\upsilon = 0$ cascade had, on the other hand, a negligible primary population. The populations in states which were not directly observed were estimated by fitting cascade models on the population evolutions of the measured states.

Information obtained from the delayed annihilation time spectrum of $\overline{p}\,^4\mathrm{He}^+$ (undisturbed by laser stimulation and measured at LEAR) [18] was also incorporated into the overall picture afforded by the laser studies. The spectrum (Fig. 4) showed that $f_{\mathrm{trap}} = (3.0 \pm 0.1)\%$ of the antiprotons survive for more than 15 ns. In the $\overline{p}\,^3\mathrm{He}^+$ case, measurements gave a value of $(2.4 \pm 0.1)\%$ [19].

In Fig. 5, the distributions of primary populations (characterized by the n and υ values) are shown. Nearly all the metastable $\overline{p}\,^4\mathrm{He}^+$ atoms lie in the region $n = 37$–40, with the $n = 38$ states containing the largest population. This appears to support the estimate $n_0 \sim 38$ given by Eq. (1). The primary populations of $\overline{p}\,^3\mathrm{He}^+$ atoms were distributed over a lower range of n values between 35 and 38, which is compatible with the estimation $n_0 \sim 37$. The sums of the individual populations in all the measured $\overline{p}\,^4\mathrm{He}^+$ and $\overline{p}\,^3\mathrm{He}^+$ states were $(3.5 \pm 0.8)\%$ and $(2.5 \pm 0.8)\%$, respectively, which account for the observed fractions of delayed annihilations described in the previous paragraph.

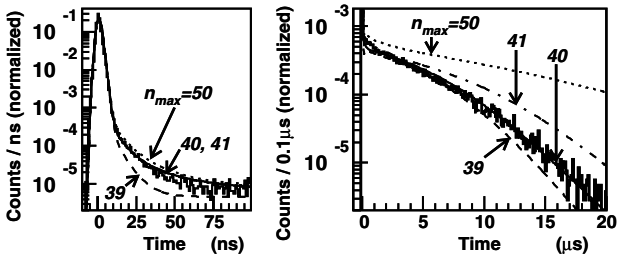

FIG. 4. Measured delayed annihilation time spectra of $\overline{p}\,^4\mathrm{He}$, compared with simulated spectra for cases where the states are populated up to $n_{\max} = 39$ (dashed lines), 40 (solid lines), 41 (dot-dashed lines), and 50 (dotted lines).

By energy conservation, the binding energy B_n of the populated atom is equal to $I_0 - T_{\overline{p}} m_{\mathrm{He}}/(m_{\mathrm{He}} + m_{\overline{p}}) + T_e$, I_0 being the ionization potential of helium ($\sim$ 24.6 eV), $T_{\overline{p}}$ and T_e the laboratory energies of the incoming antiproton and ejected electron, and m_{He} and $m_{\overline{p}}$ the helium and antiproton masses. Several theoretical calculations [20–25] (two such results are shown in Fig. 5) predict that T_e is small with respect to I_0. Only antiprotons $T_{\overline{p}} \ll I_0$ will be captured into the $n_0 \sim 37$–38 states having binding energies $B_n \sim I_0$, whereas the more energetic antiprotons ($T_{\overline{p}} \sim 25$ eV) are captured into much higher ($B_n \sim 0$) regions with n values exceeding 50. The calculations predict that $f_{\mathrm{trap}} = (12$–$25)\%$ of the antiprotons should be captured into $\overline{p}\,^4\mathrm{He}^+$ states (see Table I), with most of them in states above $n \geq 41$.

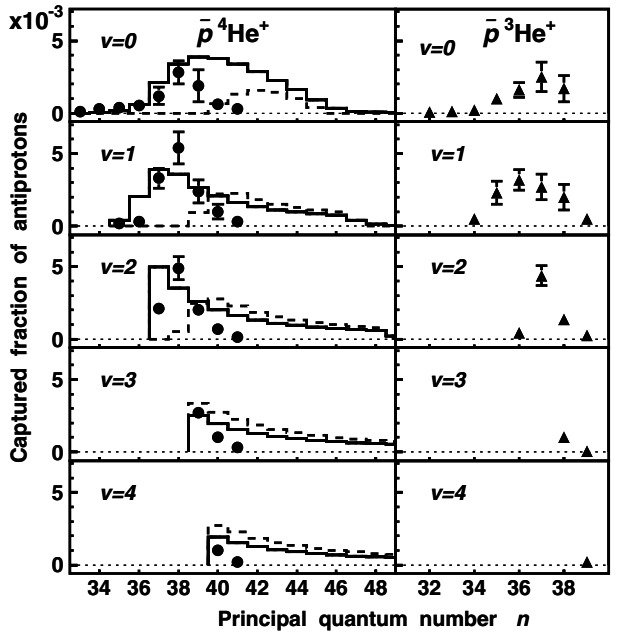

FIG. 5. Measured distributions of primary populations in $\overline{p}\,^4\mathrm{He}^+$(filled circles with error bars) and $\overline{p}\,^3\mathrm{He}^+$ (filled triangles). Theoretical $\overline{p}\,^4\mathrm{He}^+$populations derived from diabatic state [20] (solid lines) and semiclassical coupled-channel [21] (dashed lines) calculations are shown.

TABLE I. Total fractions of antiprotons captured into $\overline{p}\,^4He^+$ states, and the fractions of those captured into the $n \leq 40$ region: theoretical and experimental values. Direct theory-experiment comparison may be difficult (see text).

	Metastable population (%)	
	Total	$n \leq 40$
Diabatic state [20]	11.5	4.8
Coupled-channel [21]	23.9	1.8
Semiclassical Monte Carlo [24]	24.7	11
Fermion molecular dynamics [25]	20	
Expt.	3.0 ± 0.1	3.5 ± 0.8

As these theoretical populations do not take the effect of collisions into account, they may not be directly comparable with the values presented here, which refer to atoms thermalized by many collisions. Nevertheless, as shown in Fig. 5, the experimental data for $\overline{p}\,^4He^+$ atoms agree with the results of diabatic state calculations [20,22] in the region $n \leq 40$. We detected very little or no metastable population in the region $n \geq 41$, and due to this nonobservation the total metastable fraction was found to be $f_{\text{trap}} = 3\%$. One theoretical study [26] suggests that the $\overline{p}\,^4He^+$ created in the $n \geq 41$ states recoil with such large kinetic energies that they are rapidly destroyed by collisions. Another study [27] suggests that the quenching cross sections for the $n \geq 41$ states are large even at thermal energies due to the low activation barrier in the $\overline{p}\,^4He^+$–He potential. A recent work [28] predicts that the rates of collisional Stark transitions are several times larger in $\overline{p}\,^3He^+$ compared to $\overline{p}\,^4He^+$.

Finally, cascade calculations of $\overline{p}\,^4He$ atoms were made using the measured primary populations, in an attempt to reproduce the delayed annihilation time spectrum shown in Fig. 4. We simulated the distributions of antiprotons among the metastable states in the region $n \leq 40$ as shown in Fig. 5, and allowed them to cascade through individual states (using either the experimental state lifetimes [14,15] where available or the theoretical values [16,17]), and calculated the time elapsed until their annihilation. The simulated and measured spectra (Fig. 4) agree, including the 97% fraction of antiprotons that annihilate within 15 ns, and the 3% metastable atoms that decay with a slightly downward-bending structure having a mean lifetime of $\tau_{\text{mean}} = 3\ \mu$s. Simulated spectra for cases where the states are populated up to a maximum n value of 39, 41, and 50 are also shown, derived by appending the theoretical populations for the $n \geq 41$ states. The agreement with experiment was best for the case of $n_{\text{max}} = 40$, which supports the findings of the current study that the metastable populations in the $n \geq 41$ regions are very small.

We thank the CERN PS division for their help, and K. Ohtsuki, G. Ya. Korenman, and J. S. Cohen for many discussions. This work was supported by the Grant-in-Aid for Creative Basic Research (10NP0101) of Monbukagakusho of Japan, and the Hungarian Scientific Research Fund (OTKA T033079 and TeT-Jap-4/98).

[1] E. Fermi and E. Teller, Phys. Rev. **72**, 399 (1947).
[2] G. A. Baker, Jr., Phys. Rev. **117**, 1130 (1960).
[3] T. B. Day, Nuovo Cimento **18**, 381 (1960).
[4] R. Landua and E. Klempt, Phys. Rev. Lett. 48, 1722 (1982).
[5] G. T. Condo, Phys. Lett. **9**, 65 (1964).
[6] J. E. Russell, Phys. Rev. Lett. **23**, 63 (1969).
[7] M. Iwasaki *et al.*, Phys. Rev. Lett. **67**, 1246 (1991).
[8] T. Yamazaki *et al.*, Nature (London) **361**, 238 (1993).
[9] R. S. Hayano *et al.*, Phys. Rev. Lett. **73**, 1485 (1994); **73**, 3181(E) (1994).
[10] F. E. Maas *et al.*, Phys. Rev. A **52**, 4266 (1995).
[11] N. Morita *et al.*, Phys. Rev. Lett. **72**, 1180 (1994).
[12] M. Hori *et al.*, Phys. Rev. Lett. **87**, 093401 (2001).
[13] H. A. Torii *et al.*, Nucl. Instrum. Methods Phys. Res., Sect. A **396**, 257 (1997).
[14] M. Hori *et al.*, Phys. Rev. A **58**, 1612 (1998).
[15] F. J. Hartmann *et al.*, Phys. Rev. A **58**, 3604 (1998).
[16] V. I. Korobov and I. Shimamura, Phys. Rev. A **56**, 4587 (1997).
[17] I. Shimamura, Phys. Rev. A **46**, 3776 (1992).
[18] E. Widmann *et al.*, Phys. Rev. A **51**, 2870 (1995).
[19] B. Ketzer *et al.*, Phys. Rev. A **53**, 2108 (1996).
[20] K. Ohtsuki (private communication).
[21] G. Ya. Korenman, Hyperfine Interact. **101-102**, 81 (1996); Nucl. Phys. **A692**, 145c (2001).
[22] J. S. Cohen, R. L. Martin, and W. R. Wadt, Phys. Rev. A **27**, 1821 (1983).
[23] V. K. Dolinov *et al.*, Muon Cat. Fusion **4**, 169 (1989).
[24] W. A. Beck, L. Wilets, and M. A. Alberg, Phys. Rev. A **48**, 2779 (1993); (private communication).
[25] J. S. Cohen, Phys. Rev. A **62**, 022512 (2000).
[26] G. Ya. Korenman, Phys. At. Nucl. **59**, 1665 (1996).
[27] S. Sauge and P. Valiron, Chem. Phys. **265**, 47 (2001).
[28] J. E. Russell, Phys. Rev. A **65**, 032509 (2002).